Petrology of the volcanic rocks in north of Zavieh, south west of Karaj, Iran

Masoomeh Rafiei[1], Mohammad Ebrahimi[*], Abbas Asiabanha[2]

Corresponding author address: Department of Geology, Zanjan University, Zanjan, Iran
E-mail address: mebi65@yahoo.com

1 Department of Geology, Zanjan University,

2 Department of Geology, Qazvin International Imam Khomeini University.

Abstract

The study area is located in the north of Zavieh and southwest of Karaj. This area is part of Central Iran and the volcanic belt of Orumieh–Dokhtar. According to field observation and petrographic study volcanic rocks of the study area composed of basalt, trachybasalt, basaltic andesite, trachyandesite, dacite, ignimbrite, tuff and lapillistone. Negative anomalies of Nb -Ta, Ti, and P, positive anomaly of Pb, enrichment of large ion lithophile elements and light rare earth elements besides depletion of high field strength elements in the studied rocks indicate that their magma is generated by partial melting of mantle wedge and subsequently has undergone crustal contamination. Plots of the studied rocks on discrimination diagrams suggest an active continental margin tectonic setting for them. Sieved textured plagioclases, corroded crystals of plagioclase and pyroxene and dark rim around biotite and amphibole crystals indicate that during the crystallization and formation of these rocks there was a disequilibrium condition. Disequilibrium condition might be as a result of magma mixing, crustal assimilation and/or decrease in pressure due to rapid rising of magma.

Keywords*: petrology, volcanic rocks, disequilibrium condition, Zavieh.*

Introduction

The study area is part of Central Iran and Orumieh–Dokhtar structural zones. It lies between longitudes 50^{o} 20' E to 50^{o} 45' E and latitudes 35^{o} 25' N to 35^{o} 35' N. The oldest rocks exposed in Zavieh area are Eocene and Oligocene volcanic rocks. In south-eastern part of the study area these volcanic rocks are covered with Miocene red sandstone, conglomerate, marl and gypsifereous marl (Upper Red Formation). Quaternary terraces overlie the Upper Red Formation and Eocene volcanic rocks.

Petrography

The studied volcanic rocks consist of lava flows, pyroclastic rocks and subvolcanic rocks which have cut the volcanic rocks in the form of dyke and neck. Based on microscopic study and chemical composition the studied rocks are classified as basalt, trachybasalt, basaltic andesite, trachyandesite, dacite, ignimbrite, tuff, lapillistone, olivine dolerite, microsyenodiorite and microdiorite. Glomeroporphyritic texture (fig.1) and porphyritic texture are common in lava flows. In some lava flows amygdaloidal texture is also seen. Basaltic rocks are dark in colour and show various textures including porphyritic, glomeroporphyritic and amygdaloidal. Casts of olivine altered to iddingsite are seen in basalt (fig.2). Phenocrysts of hornblende in basaltic andesite are rimed with Fe-Ti oxide (fig.3). Fe-Ti oxides rim around hornblende might be as a result of decompression and loss of water

pressure (Best, 2003). On the other hand, magma mixing can also generate Fe-Ti oxide around hornblende crystals (Rutherford and Hill, 1993; Feely and Sharp, 1996). Meanwhile sieve textured plagioclase crystals are ubiquitous in basaltic andesite (fig.4). Decompression and rapid ascend of magma might produce sieve texture in plagioclase (Tsuchiyama, 1985). Furthermore, in many cases magma mixing might be responsible for the creation of sieve textured plagioclase crystals (Nelson and Montana, 1992; Pal et al., 2007). The texture in ignimbrite is eutaxitic. Olivine dolerite is dark in colour and show intergranular texture. In marginal parts of the neck, olivine dolerite shows glomeroporphyritic texture and seriate texture.

Petrogenesis

The representative analytical data including major oxides, minor oxides, trace elements and rare earth elements of the studied rocks are shown in table 1. Diagrams shown and discussed here are drawn based on these analytical data.

Plots of the studied rocks on Harker diagrams show relatively continuous linear trends indicating that they are comagmatic. The analytical data are plot on total alkaline versus silica diagram in order to determine their magma series (fig.5). In this diagram most of the data plot on subalkaline field. Those data plotted on subalkaline field in figure 5 lie on calc-alkaline field in AFM diagram.

Rare earth element patterns of the studied rocks are shown in figure 6. These patterns are relatively smooth and show slight negative Eu anomalies which might be as a result of plagioclase fractionation. Light rare earth elements are enriched relative to heavy rare earth elements. Light rare earth elements enrichment might indicate the high concentration of these elements in the source or low degree partial melting.

Spider diagrams of the studied rocks are shown in figure 7. Negative anomalies of Nb -Ta, Ti, and P, positive anomaly of Pb, enrichment of large ion lithophile elements and light rare earth elements besides depletion of high field strength elements in the studied rocks indicate that their magma is generated by partial melting of mantle wedge and subsequently has undergone crustal contamination. Shang et al. (2004) believed that enrichment of light rare earth elements and large ion lithophile elements relative to heavy rare earth elements and high field strength elements, besides negative anomalies of Nb-Ta and Ti in spider diagrams of igneous rocks indicate that they have formed in a subduction tectonic setting and might have undergone crustal contamination.

In order to determine the tectonic setting of the studied rocks, the analytical data are plotted on discriminant diagram of Wood (1980) and Pearce (1983). Plots of the studied rocks on Th-Ta-Hf/3 ternary discriminant diagram fall in volcanic arc basalt field (fig.8). Letters A, B, C and D refer to the fields mid ocean ridge basalts, within plate tholeiitic basalts, within plate alkali basalts and volcanic arc basalts respectively. In Th/Yb-Ta/Yb discriminant diagram, the analytical data of the studied rocks lie in active continental margin field (fig.9). Abbreviations ACM, OIA, DM, EM, Th, CA and S refer to active continental margin, oceanic island arc, depleted mantle, enriched mantle, tholeiitic, calc-alkaline and shoshonitic respectively.

Conclusion

Existence of sieve texture in plagioclase and pyroxene of the studied rocks besides other disequilibrium textures such as embayed and corroded crystals of pyroxene and plagioclase and dark rimed hornblende crystals might be as a result of magma mixing. Light rare earth elements enrichment in the studied volcanic rocks might indicate the high concentration of these elements in the source. The negative anomalies of Nb-Ta, Ti and P in the spider diagrams of the studied rocks denote that they belong to a subduction tectonic setting. Furthermore, plots of the studied rocks on discriminant diagrams confirm an active continental margin setting for them.

Table-1 representative analytical data of the studied volcanic rocks. nd refer to no data.

Sample	Z1	Z11	Z31	Z40	Z46	Z52	Z60	Z64	Z71	P65	P69	P70	P71	P72	P76	P80
Sio_2	66.68	57.76	57.43	48.57	73.23	51.32	62.13	71.92	69.20	66.08	59.89	61.11	48.82	49.71	63.70	69.08
Al_2o_3	15.1	17.21	16.18	17.02	13.61	15.64	15.38	12.68	14.22	14.23	16.13	16.63	16.34	17.44	15.8	13.78
Fe_2o_3	3.70	6.99	7.23	9.43	2.21	9.25	5.33	3.58	4.04	5.62	4.22	5.00	9.25	8.85	3.96	3.45
Mgo	0.26	3.43	2.57	7.4	0.23	5.36	1./63	0.44	0.62	0.52	0.72	1.79	7.12	4.91	1.04	0.32
Cao	1.39	6.01	4.80	8./69	0.99	3.83	3.4	1.68	0.56	1.08	4.81	4.02	9.24	8.47	3.26	1.79
Na_2o	4.51	4.32	3.51	3.76	7.6	4.11	4.05	3.65	5.4	4.06	3.37	3.76	3.69	3.1	3.64	3.46
K_2o	5.08	1.25	4.59	1.10	0.05	3.98	3.47	4.3	3.52	5.24	4.88	4.14	1.26	1.23	4.25	5.28
Tio_2	0.68	0.77	0.91	1.32	0.46	0. 96	0.53	0.45	0.5	0.98	0.65	0.62	1.44	0.91	0.53	0.63
P_2o_5	0.13	0.29	0.35	0.39	0.1	0.3	0.17	0.1	0.13	0.23	0.25	0.22	0.38	0.25	0.13	0.08
Mno	0.11	0.13	0.17	0.14	0.03	0.29	0.11	0.08	0.06	0.08	0.09	0.09	0.14	0.17	0.17	0.09
Ba	1000	725	731	273	21	781	767	946	573	1692	968	927	327	475	873	954
Sr	214	558.8	380.4	751	79	290	390	244	69	221.5	338.8	406.6	769.6	636	299.4	155.8
Zr	346	144.3	244.7	166	185	127	169	182	329	289.5	152.8	134.9	148.1	64.9	182.2	240.2
Y	41	25.9	31.5	19	29	26	26	35	44	45.5	19.4	19	21.3	19.7	26.8	37.4
Nb	21	9.5	17.9	23	6	7	<5	9	13	18.4	12.7	9.9	27.8	4.9	9.1	15.5
Sc	11	18	20	21	10	26	11	10	8	15	9	12	26	25	8	11
LOI	1.3	1.6	1.8	1.2	1.3	4	3.2	0.8	1.6	1.3	4.5	2.1	1.8	4.5	3.3	1.6
Co	nd	183	15.5	nd	nd	nd	nd	nd	nd	4.2	7.1	9.2	33.2	25.7	5.2	2.7
Cs	nd	3.2	1.7	nd	nd	nd	nd	nd	nd	1.4	2	1.9	0.4	0.8	2.1	3.3
Ga	nd	16	15.2	nd	nd	nd	nd	nd	nd	17.2	14.9	16.2	18.7	18.3	17	15
Hf	nd	4	6.4	nd	nd	nd	nd	nd	nd	8.1	4	3.6	3.8	1.8	5.3	6.9
Rb	nd	83.9	111.6	nd	nd	nd	nd	nd	nd	127	156.1	121.7	16.9	21.6	120.9	143.3
Sn	nd	2	3	nd	nd	nd	nd	nd	nd	2	1	1	2	1	2	2
Ta	nd	0.7	1.2	nd	nd	nd	nd	nd	nd	1.1	0.9	0.7	1.4	0.2	0.6	0./9
Th	nd	5. 5	10.8	nd	nd	nd	nd	nd	nd	9.4	15	10.3	5.9	1.5	6.2	10.1
U	nd	1.8	3.2	nd	nd	nd	nd	nd	nd	2.8	3.4	2.9	1.3	0.5	2.1	2.6
V	nd	154	128	nd	nd	nd	nd	nd	nd	40	66	98	169	203	51	21
W	nd	0.8	1.4	nd	nd	nd	nd	nd	nd	3.8	3.1	3.6	4	1.2	2.2	4.3
La	nd	26. 7	33.2	nd	nd	nd	nd	nd	nd	30.7	25.7	24.6	31.9	14.4	24.2	28.5
Ce	nd	48. 2	60.5	nd	nd	nd	nd	nd	nd	69.5	50.4	46.3	64.3	30.4	49.2	60.3
Pr	nd	6.66	8.7	nd	nd	nd	nd	nd	nd	8.15	5.33	5.02	6.83	3.65	5.51	7.11
Nd	nd	25.7	31.3	nd	nd	nd	nd	nd	nd	37/8	21.2	20.3	27.9	16.4	24.6	31.2
Sm	nd	4.82	6.78	nd	nd	nd	nd	nd	nd	7.9	3.8	3.9	5.1	3.7	4.7	5.9
Eu	nd	1.42	1.57	nd	nd	nd	nd	nd	nd	1.58	1.01	1.03	1.55	1.19	1.29	1.46
Gd	nd	4. 98	6.64	nd	nd	nd	nd	nd	nd	6.97	3.42	3.36	4.01	3.41	3.9	5.8
Tb	nd	0.77	1.04	nd	nd	nd	nd	nd	nd	1.33	0.59	0.52	0.65	0.57	0.68	0.98
Dy	nd	4.53	5.74	nd	nd	nd	nd	nd	nd	7.85	3.26	3.22	3.8	3. 26	4.31	5.65
Ho	nd	0.91	1.23	nd	nd	nd	nd	nd	nd	1.65	0.67	0.68	0.71	0.65	0.9	1.22
Er	nd	2.74	3.34	nd	nd	nd	nd	nd	nd	4/56	1/78	1/81	1/92	1/91	2. 56	3.78
Tm	nd	0.43	0.54	nd	nd	nd	nd	nd	nd	0/74	0/3	0/29	0/29	0.29	0.43	0.56
Yb	nd	2.61	3.33	nd	nd	nd	nd	nd	nd	4.98	1.9	2.05	1.78	1.96	2/67	3.82
Lu	nd	0.42	0.52	nd	nd	nd	nd	nd	nd	0.7	0.27	0.28	0.26	0.23	0.43	0.55
Mo	nd	0.7	1.6	nd	nd	nd	nd	nd	nd	1	2.4	2	1.6	0.2	0.8	1.3
Cu	nd	47.4	9.1	nd	nd	nd	nd	nd	nd	6.5	10.5	22.1	31.5	39.4	13.7	6
Pb	nd	1.3	36	nd	nd	nd	nd	nd	nd	8.6	5.7	3.7	1.5	2.7	14.8	8.7
Zn	nd	33	136	nd	nd	nd	nd	nd	nd	70	42	44	69	60	31	34
Ni	nd	7.1	8.9	nd	nd	nd	nd	nd	nd	4.1	2.1	4.2	75.5	17.5	1.8	2.6

Fig.2 Iddingsite pseudomorphose after olivine in basalt.

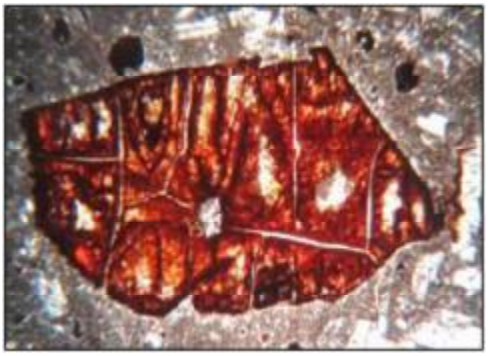

Fig.1 Glomeroporphyritic texture in trachybasalt.

Fig.4 Sieve textured plagioclase in basaltic andesite.

Fig.3 Dark rimed hornblende in basaltic andesite.

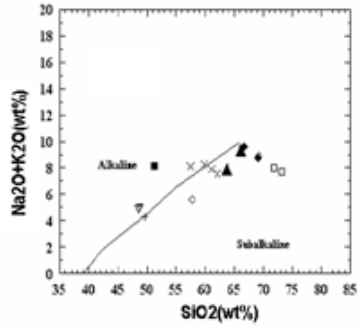

Fig.5 Total alkaline versus silica diagram forthe studied rocks. The dividing line is fromIrvine and Baragar (1971).

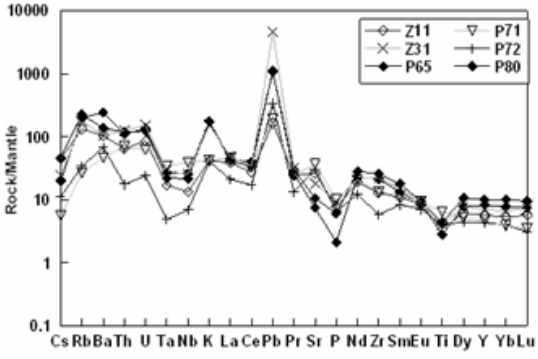

Fig.7 Spider diagrams for the studied rocks. Normalising factors after McDonough et al. (1991).

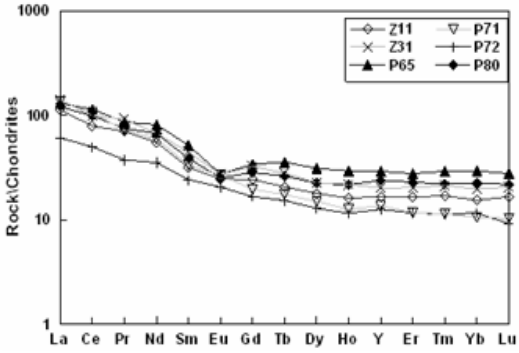

Fig.6 Normalised REE patterns for the studied rocks. Normalising factors after McDonough et al. (1991).

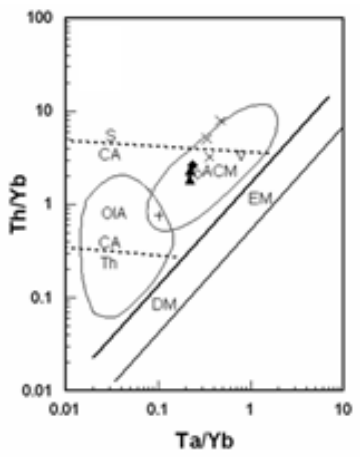

Fig.9 Plots of the studied rocks on discriminant diagram of Pearce (1983).

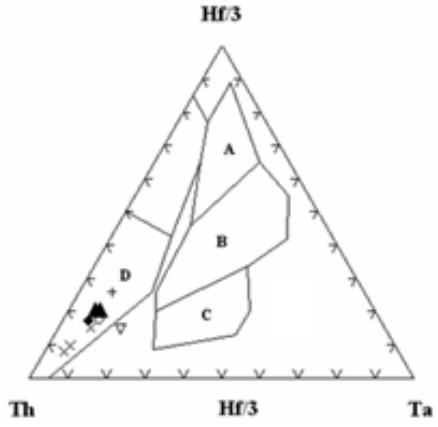

Fig.8 Plots of the studied rocks on discriminant diagram of Wood (1980).

Reference

1- Best, M.G., 2003, Igneous and metamorphic petrology: Blackwell Publishing 729 p.

2- Feely, T.C., and Sharp, I.D., 1996, Chemical and hydrogen isotope evidence for in situ dehydrogenation of biotite in silicic magma chambers: Geology, v. 24, p. 1021-1024.

3- Irvine, T.N., and Baragar, W.R.A., 1971, a guide to the chemical classification of the common volcanic rocks: Canadian Journal of Earth Sciences, v. 8, p. 523-548.

4- McDonough, W.f., Sun, S., Ringwood, A.E., Jagoutz, E., and Hofmann, A.W., 1991, K, Rb and Cs in the earth and moon and the evolution of the earth mantle: Geochemical et Cosmochemical Acta, Ross Taylor Symposium volume.

5- Nelson, S.T., and Montana, A., 1992, Sieve textured plagioclase in volcanic rocks produced by rapid decompression: American Mineral, v. 77, p. 1242-1249.

6- Pal, T., K.Mitra, S., Sengupata, S., A.Katari, P.C., Padhyay, B., and Bhattacharya, A., 2007, Dacite-Andesite of Narcodam volcano in the Andaman Sea- An imprint of magma mixing in the inner arc of the Andaman-Java subduction system: Journal of volcanology and Geothermal Researches, v. 168, p. 93-113.

7- Pearce, J.A., 1983, the role of subcontinental lithosphere in magma genesis at destructive plate margins in continental basalts and mantle xenoliths: Hawkesworth, C.J., and Norry, M. G., (eds): Nantwich: Shiva, p. 230-249.

8- Rutherford, M.J., and Hill, P.M., 1993, Magma ascent rates from amphibole breakdown: an experimental study applied to the 1980-1986 Mount St.Helens eruptions, Journal of Geophysical Researches, v. 98, p. 19667-19685.

9- Shang, C.K., Satir, M., Nsifa, E.N., Taubald, H., Liegeois, J.P., and Tchoua, F.M., 2004, Geochemistry, Rb-Sr and Sm-Nd systematic: case of the Sangmelima region, Ntem complex, south Cameroon: Journal of African Earth Sciences, v. 40, p. 61-79

10- Tscuchiyama, A., 1985, Dissolution kinetics of plagioclase in the melt of the system diopside-albite - anorthite and origin of dusty plagioclase in the andesites: Contribution to Mineralogy and Petrology, v. 89, p. 1-16.

11- Wood, D.A., 1980, the application of a Th-Hf-Ta diagram to problems of tectonomagmatic classification and to establishing the nature of crustal contamination of basaltic lavas of the British Tertiary volcanic province: Earth Planetary Science Letters, v. 37, p. 90-96.